One step toward automating vessel detection and labeling in the neck for flow quantification

Ying Wang[1,2], Jing Jiang[1,3], Paul Kokeny[1], Yi Zhong[4], and E. Mark Haacke[1,4]

[1]Department of Biomedical Engineering, Wayne State University, Detroit, MI, United States, [2]College of Information Science and Engineering, Northeastern University, Shenyang, Liaoning, China, [3]Department of Radiology, Wayne State University, Detroit, MI, United States, [4]MR Innovations, Inc., Detroit, MI, United States

Purpose: Magnetic resonance imaging (MRI) has played a critical role in studying neurovascular diseases such as stroke, multiple sclerosis (MS), traumatic brain imaging (TBI), Parkinson's disease (PD) and vascular dementia [1]. Phase contrast MR imaging (PCMRI) makes it possible to quantify blood flow patterns for the major vessels. This requires vessel segmentation and identification which is usually done manually. This can be time consuming and, being observer-dependent, may lead to significant variation. Automatic segmentation and labeling would eliminate such subjectivity however several challenges arise. The Common Carotid Arteries (CCA) and Internal Jugular Veins (IJV) run side-by-side in the neck and has been shown to cause the inadvertent CCA identification while targeting the IJV, with an incidence of 2%-8% [2, 3]. Automatic methods have been explored for MRI and other imaging modalities as well [4-6]. Other vessel segmentation algorithms based on deformable models, k-means clustering, and region growing are among the most investigated [7-13] are more for the segmentation purpose and lack of the identification part. Our recent work on Tissue Similarity Mapping (TSM) [14] that exploits the temporal signal behavior can be used to segment and identify vessels in the neck.

Methods: The overall workflow of our proposed method consists of the flowing steps: (1) *Remove the noise and background by Otsu method from a time-averaged magnitude image*. A cost calculation based on Otsu segmentation [15] is used to find a threshold that separates the bright vessels and hypointense static tissues in the time-averaged magnitude image; (2) *calculate the velocity maps from phase images*. The user is required to draw the non-flow-area (NFA) in the muscle area to compensate for any background phase shift; (3) *calculate the TSM to enhance vessel differentiation from background tissue.* The NFA area drawn will be used as reference to calculate the mean squared error (MSE) for each pixel, where each error is the difference in signal between a pixel and the reference area at a time point. . This will make the any tissues with no flow appear hypointense (low MSE) while the vessels will appear hyperintense (high MSE), shown in Figure 2A; (4) *auto select the reference artery and vein by the highest mean velocity;* Otsu separation and connectivity are performed on the TSM image to create a collection of connected elements (potential vessels). The element with the highest mean positive velocity will be chosen as the reference artery while the highest mean negative velocity will be chosen as the reference vein; (5) *calculate blood volume maps (BVM) by using the reference artery and vein;* The BVMs are calculated by generating normalized velocity TSM maps from both the reference artery and vein; (6) *generate the artery and vein masks;* the BVMs are thresholded and multiplied with the mean of the magnitude images. This will generate the arteries and veins separately, shown in Figure 2B and 2C; (7) *label the vessels*. The vessel location and size information at the C6 level will be used to label the vessels separately in the masks of arteries and veins. Labelled results are displayed on top of the input vessel in Figure 1. Segmentation is inherently part of the labeling process, thus once finished, flow can be quantified for each vessel. This method was performed on 7 human PC-MRI data sets and used to identify and quantify 10 different vessels at the C6 level of the neck (left and right CCAs, IJVs, external jugular veins (EJVs), vertebral veins (VVs), and vertebral arteries (VAs)). To test the accuracy of the segmentation and labeling, 3 experienced PC-MRI data processors were asked to perform 2 trials of manual segmentation on the same 7 data sets. The similarity index was calculated for every processor's pair of trials as a means to eliminate any inconsistent results, although none were found. One processor's segmentation results were chosen for each case based on visual examination. Segmentation accuracy was evaluated by comparing the flow quantification results while labeling accuracy was evaluated by simply comparing labels.

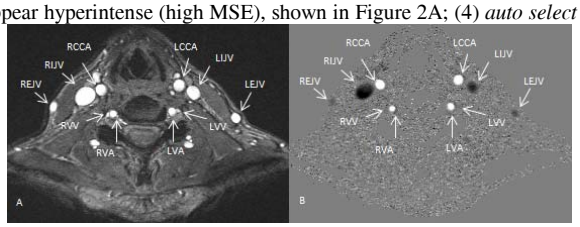

Figure 1: (A) Magnitude (B) vessel identification on phase image

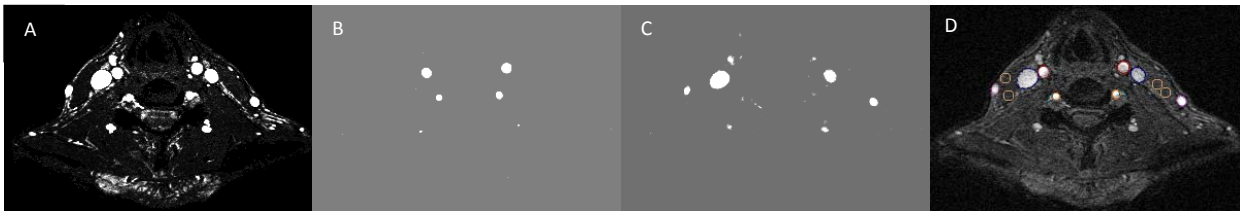

Figure 2: Output of the result (A) after TSM to enhance vessels in step (3); (B) of Arteries mask and (C) veins mask in step (6); (D) segmentation boundary.

Case #	L-VV	R-VV	L-EJV	R-EJV	L-IJV	R-IJV	L-VA	R-VA	L-CCA	R-CCA
1	N/A	N/A	3.9	1.8	0.2	0.4	1.1	0.4	0.7	0.2
2	3.6	2.1	0.8	0.2	1.1	3.4	0.3	0	2.9	6.1
3	1.9	25.5	1.9	1.3	1.1	1.3	0.5	0.8	0.6	0.4
4	N/A	1.9	5.8	5.2	1.1	1.1	2.5	2.7	1.1	0.8
5	1.3	N/A	1.4	0.6	0.8	0.4	0.3	3.4	0.2	0.6
6	0.2	4.4	9	1.5	28	5.4	4.5	1.5	6.9	6
7	3.2	9.2	6.4	9.2	3	2.4	6.5	1.9	1	0.8

Table 1: Percent difference of the average flow rate between the auto segmentation and the manual segmentation

Results: All manually identified vessels were correctly identified by our automatic algorithm for all 7 data sets. The error in average flow rate for each identifiable vessel of each case are shown in Table 1. The VVs were not identified manually in 3 of the data sets. All errors were under 10% except the R-VV in case 3, which was less than 3 pixels in diameter and thus is highly sensitive to differences in segmentation, and L-IJV in case 6 which suffered from severe aliasing that caused the segmentation algorithm to miss part of the vessel.

Conclusion: The proposed automatic vessel identification and segmentation algorithm can save processing time and was shown to successfully identify all ten vessels of interest in the C5/C6 location, distinguishing between the CCA and IJV even when they are side by side and appear as one connected structure in the magnitude image.

References: [1] Feinberg, et al. MRM. 1985; 2(6): 555-566. [2] D. MJ, et al. ANAESTH INTENS CARE. 1982; 10(1), 9-14. [3] Patel C, et al. Crit Care Med. 1986; 14(3):195-7 [4] D. Wang, et al. MICCAI. 2006; 654-661. [5] M. Schneider, et al. IEEE. 2010; 45-48. [6] Da-Chuan Cheng, et al. BME Online. 2011. [7] Thierry Yzet , et al. EJR. 2010; 73, 119–124. [8] O.Baledent, IR. 2001; 36, 368–377. [9] S.Kozerke, JMRI. 1999; 10, 41–51. [10] A.Herment, et al. JMRI. 2010; 31(4), 881-888. [11] Kirbas, C., et al. ACM COMPUT SURV. 2004; 36(7), 81-121. [12] Oelhafen, M., et al. JMRI2. 2006; 23(3), 422-429. [13] Yan, P., et al. MIA. 2006; 10(3), 317-329. [14] E. Mark Haacke, et al. MRI. 2013; 31, 481–489. [15] Otsu N. IEEE T SYS MAN CYB Man. 1979. **Acknowledgement**: Research reported in this publication was supported by the NHLBI of the NIH under Award Number R42HL112580.